Influence of polyaluminum chloride self-aggregation on flocculation performance

Karen A Swetland[a], Monroe L Weber-Shirk[a,*], Leonard W Lion[a]

[a] *School of Civil and Environmental Engineering, Cornell University, Ithaca, NY 14853, USA*

Abstract

Polyaluminum chloride (PACl) is a commonly used coagulant for water treatment. One mode of action of PACl ($(AlO_4Al_{12}(OH)_{24}(H_2O)_{12})^{7+}$) is reported to be through formation of aggregates that bridge between colloids. Although many studies have considered the effectiveness of PACl under a spectrum of conditions for influent suspensions, little is known about the rate of formation of PACl aggregates upon mixing with influent water and the effect of aggregate size on the subsequent formation of flocs that can be readily removed by sedimentation. PACl aggregates larger than $0.18\,\mu m$ in diameter were formed under controlled conditions. A kinetic aggregation model was developed and validated to give the aggregate size before mixing with a colloidal suspension and entering a flocculator. After flocculation, the ensuing floc sedimentation velocity and residual turbidity were non-destructively observed. Experimental and modeling results combined with geometric analysis show that, under the experimental conditions tested in this research, PACl self-aggregation consistently lowers attachment efficiency of the colloidal suspension, reduces the effectiveness of the flocculator, and reduces turbidity removal. Minimization of PACl aggregate size is best accomplished by immediate, rapid, and efficient mixing of PACl with the influent water. The relationship between residual turbidity and PACl dose is consistent with expectations based on a geometric adhesive model of coagulation.

Keywords: Rapid mix; PACl; coagulation; flocculation; aggregation; surface coverage;

1. Introduction

In water treatment, coagulation and flocculation are used to form particle aggregates or flocs that can be subsequently removed by sedimentation or filtration. Coagulation increases attachment efficiency, i.e., the fraction of particle collisions that result in aggregation.. Flocculation is the transport phase in which the particles collide and aggregate [2]. While coagulation in drinking water treatment always involves the addition of a coagulant, the particular chemical, dose, and other relevant conditions determine the attachment efficiency and the ensuing success of coagulation. .

1.1. PACl Structure and Precipitation

Polyaluminum chloride (PACl) is an inorganic polymer coagulant that has gained wide acceptance for use in water treatment as a result of its efficacy over a broader pH range and at lower temperatures than the commonly used alternative, aluminum sulfate (alum) [3]. PACl is commonly prepared by the controlled neutralization of aluminum chloride. The dominant stable species in dissolved PACl, $(AlO_4Al_{12}(OH)_{24}(H_2O)_{12})^{7+}$, commonly referred to as Al_{13}, has a Keggin-13 structure and a hydrated radius of $1.2\,nm$ [28]. When the dose of coagulant exceeds the solubility limit, precipitation occurs. PACl precipitates, or aggregates, are composed of Al_{13} subunits. Benschoten and Edzwald [3] proved through timed spectrophotometry that the precipitation products of alum and PACl were characteristically different and that PACl precipitates retained their polymeric structure.

Many mechanisms have been proposed for coagulation of suspensions by PACl including: (1) Destabilization of colloidal particles by the nucleation of positively charged Al_{13} precipitates on negatively charged colloidal surfaces, or precipitation charge neutralization (PCN) [**?**]. PCN is based on the observation that,

*Email: mw24@cornell.edu Phone: 1 607 255 8445 Fax: 1 607 255 9004

under the circum-neutral pH of most natural waters, the precipitates of aluminum salts and polymers are positively charged. These species are thought to destabilize negatively charged colloids by attaching and neutralizing their surface charge, thereby decreasing electrostatic repulsion between colloids and inducing aggregation [28]. (2) As a consequence of the relatively large size and stability of PACl aggregates and their positive charge, electrostatic patch coagulation (EPC) has also been proposed as a potential coagulation mechanism [28]. EPC is characterized as a localized precipitation charge neutralization mechanism; patches of positive charge are created by aggregates of coagulant adsorbing to a small fraction of the surface of the colloid. Attractive electrostatic forces then attach the positively charged PACl patches to the "naked" surface of other colloids upon collision. It is hypothesized that large flocs can be formed in this manner [10, 28, 11]. (3) At high coagulant doses, colloidal particles can be removed when they become enmeshed in the voluminous self-aggregated coagulant precipitate, a process called "sweep flocculation"[2]. The term sweep flocculation is best thought of as a description of the colloid and coagulant suspension and does not provide a mechanistic understanding of why precipitated coagulant should interact with itself or colloids in the observed manner. Sweep flocculation is observed at coagulant doses that are higher than are commonly used in water treatment. Consequently, EPC and PCN are explored in more detail below.

1.2. DLVO Theory and Model

The interaction between charged particles in a suspension is cited as the driving mechanism in PCN and EPC and has been modeled by the Derjaguin-Landau-Verwey-Overbeek (DLVO) theory. In this model, Van der Waals interactions are responsible for the attractive force between particles, V_A. V_A is inversely proportional to separation distance between particles and is therefore effective at small separation distances (Equation 1) [21].

$$V_A = \frac{-A_H a}{12h} \tag{1}$$

where A_H is the Hamaker constant, a is the radius of the particle, and h is the distance between the particles.

Repulsive forces in the DLVO model, V_R, originate when the similarly charged electrical double layers of particles overlap and are proportional to the surface charge squared (Equation 2).

$$V_R = 2\pi\epsilon a\zeta^2 exp\left(-\kappa h\right) \tag{2}$$

where ϵ is the dielectric constant of water at 298K, ζ is the zeta potential of the particle (see Section 1.3 for more detail), and κ is the inverse of the Debye-Huckel length and is given by Equation 3.

$$\kappa = \left(\frac{2e^2 N_A I}{\epsilon k_B T}\right)^{1/2} \tag{3}$$

where e is the elementary charge of an electron, N_A is Avogadro's number, I is the ionic strength of the solution, k_B is Boltzmann's constant, and T is the temperature.

Attractive and repulsive forces between particles can be summed to find the total force, V_T (Equation 4). When V_T is positive (V_R dominates), the area under the curve of V_T as a function of separation distance represents the activation energy, the energy that must be provided to allow two particles to get close enough so that the attractive Van der Waals force dominates.

$$V_T = V_R + V_A \tag{4}$$

Application of the DLVO theory to a colloidal suspension suggests that the electrostatic destabilization of colloidal suspensions occurs when the activation energy is reduced so colloids can approach one another. According to PCN and EPC, the goal of coagulation is the electrostatic destabilization of the colloidal suspension. Electrostatic destabilization can be achieved by changing the surface charge of the colloids, which is incorporated into the DLVO theory by zeta potential, ζ, or through reducing the distance over which repulsive forces act by increasing the ionic strength, I, of the solution. The addition of positively charged coagulant aggregates that adsorb/attach to the surface of the colloid would reduce the surface charge and the resulting energy barrier. Electrostatic attraction would hold the PACl aggregates to the colloidal surface, and the Van der Waals forces accounted for in DLVO theory would be responsible for the inter-particle bond that holds the charge-neutralized colloidal particles together [13].

Figure 1 depicts the interaction energy of a suspension of kaolin clay at the solution conditions used for experiments in this research. DLVO theory suggests that kaolin clay particles in Cornell tap water would be able to aggregate with a spacing between particles of 10 nm because the van der Waals attractive force exceeds the electrostatic repulsive force at that separation distance. However, a kaolin suspension in Cornell tap water does not create flocs with sedimentation velocities that enable removal in a sedimentation tank without the addition of a coagulant (Figure 5 at $0\,\frac{mg}{L}$ coagulant dose). The inability of the DLVO theory to predict the failure of kaolin clay to aggregate suggests that an additional mechanism is important in determining the aggregation behavior of colloids undergoing flocculation.

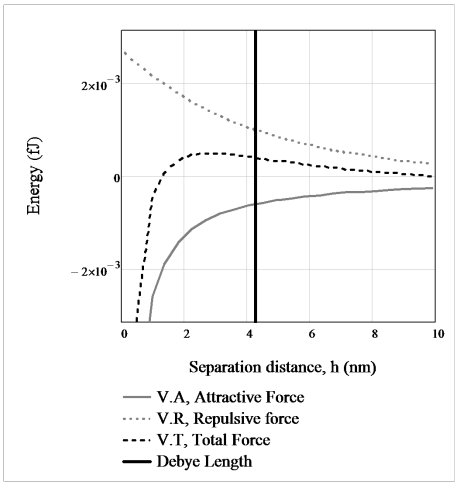

Figure 1: Interaction energy for $30\,\frac{mg}{L}$ kaolin clay in Cornell tap water, $\kappa = 0.237\,nm^{-1}$, $a = 1\,\mu m$, $\zeta = -25\,mV$, $0\,\mu M$ Al.

1.3. Measuring charge

Precipitation-charge neutralization (PCN) is hypothesized to facilitate aggregation when the colloid's negative surface charge is near neutral. Surface charge, the electrical charge present at the surface, should be measured as a surface potential, the difference between the electrical potential of the surface and the bulk fluid (outside the electrical double layer). However, counter-ions and water molecules that are strongly bound to the surface of the charged particle interfere with a direct measurement. Zeta potential is the difference in electrical potential between the shear plane and the bulk fluid and is used as a surrogate parameter for surface potential [21]. The shear plane is defined as the position where bulk fluid can slip by a moving particle; fluid within the shear plane moves with the particle due to intermolecular forces. It has long been assumed that the shear plane lies near the Stern layer, the monolayer of positive ions from the solution that are attracted to the colloid surface, approximately $0.5\,nm$ from the surface of the colloid. Li et al. [8] determined the shear plane's distance from the surface to be approximately the the same as the Guoy plane. The Guoy plane is defined by electrochemical composition and is located one Debye length from the colloid surface. The volume created one Debye length ($20 - 30\,nm$ in a $10^{-4}M$ 1:1 electrolyte solution, and $4.2\,nm$ in the Cornell tap water used for this study) from the surface of the colloid is the volume containing sufficient excess ions of opposite charge to counter act the charge of the particle. It should be noted that while EPC and PCN are based on electrostatic charge neutralization, zeta potential is not an appropriate parameter for determining the coagulant dose at which EPC will be effective because zeta potential is averaged over the whole surface of the colloid.

1.4. Diffusion Limited & Reaction Limited Colloid Aggregation (DLCA & RLCA)

Aggregation often begins with a suspension of mono-disperse particles that collide and form clusters due to Brownian motion [1, 13]. These clusters continue colliding due to both Brownian motion and velocity gradients resulting in a suspension of polydisperse clusters. Through static and dynamic light scattering experiments, researchers have found that the aggregation kinetics of many different colloids follow the same

pattern [13]. As a result, colloidal aggregation kinetics have been conceptually divided into two distinct stages - diffusion limited (DLCA) and reaction limited colloid aggregation (RLCA). In DLCA, the aggregation rate is limited only by the rate of collisions between the particles; this assumes an attachment efficiency near unity. To predict an attachment efficiency near unity for DLCA, the repulsive barrier between two approaching particles must be reduced to much less than k_BT, an approximation of the Brownian energy. If the energy barrier is reduced to near zero, the full extent of DLCA can be achieved. In RLCA, collisions are driven by velocity gradients and multiple collisions are required before two particles can stick together (attachment efficiency less than one) resulting in a slower aggregation rate. In all stages of colloid aggregation, the clusters of original colloids (primary particles) take on a fractal structure, with a fractal dimension $d_f \approx 1.8$ for DLCA and $d_f \approx 2.1$ for RLCA [13, 1?].

1.5. PACl Self-Aggregation Model (DLCA & RLCA)

To interpret the impact of PACl self aggregation on flocculation, a physically-based model was generated to capture the kinetics of Al_{13} self-aggregation in a circum-neutral pH suspension in the absence of other colloids. The primary PACl molecule ($(AlO_4Al_{12}(OH)_{24}(H_2O)_{12})^{7+}$) is estimated to be $1.2\,nm$ in diameter [17]. However, because of its propensity to self-aggregate, PACl is rarely observed as individual molecules. PACl obtained from suppliers has already undergone some self aggregation. Therefore, the initial diameter, $d_{initial}$, used in the model was not the diameter of a single PACl molecule, but rather the observed average particle size, $180\,nm$ (determined using a Malvern Zetasizer Nano-ZS, for the PACl used in this research obtained from Zhengzhou City Jintai Water Treatment Raw Material Co., Ltd.). The model provides an estimate of the final size of a PACl aggregate after a specified period of mixing due to collisions resulting from both diffusion and shear (Equation 20).

To account for the fractal nature of aggregates [11, 1, 16, 23], a fractal growth equation was used to determine size of the aggregate particle after each consecutive collision (Equation 5). Inherent in this equation is the assumption that all collisions occur between identical particles; such that collisions double the number of the primary particles within the resulting aggregate.

$$d_n = d_{initial} 2^{\frac{n}{D_{Fractal}}} \tag{5}$$

where n is the number of sequential collisions, $D_{Fractal}$ is the fractal dimension, d_n is the aggregate diameter after n collisions, and $d_{initial}$ is initial aggregate diameter. The initial floc volume fraction, $\phi_{initial}$ is calculated by (Equation 6).

$$\phi_{initial} = \frac{C_{PACl}}{\rho_{initial}} \tag{6}$$

where C_{PACl} is the concentration of PACl in the PACl aggregation tube used in this research, and $\rho_{initial}$ is the observed density of PACl, $1.138 \frac{gm}{mL}$ (see Section 1.6). The floc volume fraction for a given collision, ϕ_n, is then calculated as (Equation 7):

$$\phi_n = \phi_{initial} \left(\frac{d_n}{d_{initial}} \right)^{3-D_{Fractal}} \tag{7}$$

The effective particle density number, N_n, is determined by dividing the floc volume fraction by the volume of a single aggregate (Equation 8).

$$N_n = \frac{\phi_n}{\frac{\pi}{6} d_n^3} \tag{8}$$

Given N_n, the model of Meibodi et al. [15] that assumes Brownian motion and uses the Smoluchowski approach for the collision of particles in a dilute suspension is used to calculate the average time for a given collision, n, ($t_{n,diffusive}$) (Equation 9).

$$t_{n,diffusive} = \frac{3\nu}{8 k_B T N_n} \tag{9}$$

where ν is the dynamic viscosity of water at $298\,K$. Because of the initial $180\,nm$ aggregate size and concentration used in experiments, shear induced collisions also occur in the reactor and contribute significantly

to the final aggregate size. Shear induced collisions are considered RLCA in nature and have an attachment efficiency less than unity. The time for a shear induced collision can be modeled by Equation 10, as derived by Weber-Shirk and Lion [23].

$$t_{n,shear} = \frac{1}{6}\left(\frac{6}{\pi}\right)^{\frac{1}{3}}\left(\frac{\nu}{\varepsilon}\right)^{\frac{1}{2}}\frac{1}{\phi_n^{\frac{2}{3}}} \tag{10}$$

In the transitional range between DLCA and RLCA, diffusion and shear transport processes act in concert to cause collisions. Equation 11 calculates the collision time when both transport mechanisms are operative.

$$t_n = \frac{1}{\frac{1}{t_{n,diffusive}} + \frac{1}{t_{n,shear}}} \tag{11}$$

Each collision time is subtracted in the model from the total experimental reaction time available. Total reaction time was controlled in experiments through laminar flow in a microbore tube of defined length and diameter. When the available reaction time is depleted, the number of collisions is used in the fractal growth equation (Equation 5) to give the final aggregate size. The number of sequential collisions was not limited to integer values to obtain the best estimate of the average aggregate size.

The model for diffusion limited PACl aggregate growth was validated experimentally using a Malvern Zetasizer Nano-ZS. A $5\,mM\,Al$ suspension of PACl aggregates was filtered through a $0.2\,\mu m$ syringe filter to isolate a narrow size distribution so as to reduce variability in the observed sizes during aggregation. After filtration, initial aggregates were $55\,nm$ in diameter. As expected, this is less than the average aggregate size in the unfiltered suspension, $180\,nm$. The suspension pH was adjusted to 7.5 by addition of dilute Na_2CO_3 and a series of size measurements was taken (final PACl concentration $2.5\,mM\,Al$). The sample cell was not mixed during the measurement phase and thus the only transport mechanism for collisions was Brownian motion. Observations of aggregate size immediately after pH neutralization were not obtained because initial collisions occurred at a time scale faster than the start-up detection time required for the Zetasizer ($10\,s$). However, even with the difficulties inherent in observing particle collisions over very short time and length scales, the results (Figure 2) suggest that the model based on DLCA is consistent with the observed self-aggregation for PACl.

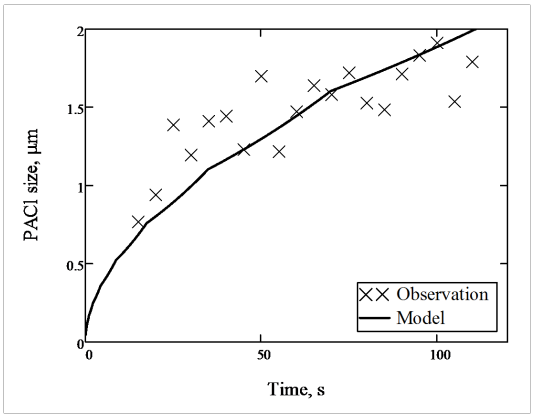

Figure 2: Diffusion limited PACl self-aggregation as a function of time at a neutral pH. PACl concentration was $2.5\,mM\,Al$. Measurements exhibit variability because of the polydisperse character of the suspension and because averaging of size measurements was eliminated to decrease the time interval between measurements. The model assumes a fractal dimension of 1.85 for DLCA in the quiescent sample and an initial particle size of $55\,nm$. $R^2 = 0.69$, $n = 20$

1.6. Coagulation Geometries

A careful geometric analysis for the attachment of coagulant particles to colloid surfaces can enlighten our understanding of the role of the coagulant on subsequent colloid aggregation. The effectiveness of PACl

as a coagulant for negatively charged kaolin clay particles is generally attributed to charge neutralization based on its high positive charge density [26, 10, 3, 28, 25, 12]. However, if the diameter of PACl coagulant aggregates exceeds the Debye length, there is no reason to expect charge neutralization to be a prerequisite of aggregation. This is consistent with observations by Chu et al. [4], Wu et al. [25] of flocculation with negative zeta potential (see Section 1.7).

As an initial approximation, kaolin clay platelets were assumed to have the volume of a sphere with a diameter of $2\,\mu m$ [28, 10]. The platelets were assumed to be cylinders with a 10:1 diameter to height ratio, resulting in a diameter of $3.8\,\mu m$, height of $0.38\,\mu m$, and an initial surface area of $27\,\mu m^2$. The geometries used in Figure 3a correspond to a turbidity of 15 NTU ($30\,mg/L$ clay, relationship determined through laboratory observations) and a PACl concentration of $14.4\,\mu M\,Al$, at a pH of 7.5. The number of clay particles present assumes the density of kaolin clay, ρ_{Clay}, is $2.65\,\frac{gm}{mL}$. If initial PACl aggregate diameters are close to $180\,nm$ with a fractal dimension of 2.9 due to aggregation and dehydration that occurred during the manufacturing process (as was the case for the PACl used in this research) the precipitated PACl would cover 14% of the clay surface on average (Figure 3a) [14, 3]. This calculation assumes that all PACl molecules above the solubility limit precipitate and attach to a clay platelet. At pH 7.5 the solubility limit of PACl is $82\,nM\,Al$ [3]. If the coagulant is allowed to self-aggregate at circum-neutral pH for 6.2 s under the conditions in this study, $1\,\mu m$ aggregates are formed (see aggregation model below), covering only 4% of the colloid surface (Figure 3b). For comparison, the Debye length corresponding to the ionic strength ($I = 5.2\frac{mol}{m^3}$) of Cornell University tap water is $4.2\,nm$. This coupled geometric and DLVO analysis suggests that charge neutralization may not be relevant for PACl dosages typically used in drinking water treatment.

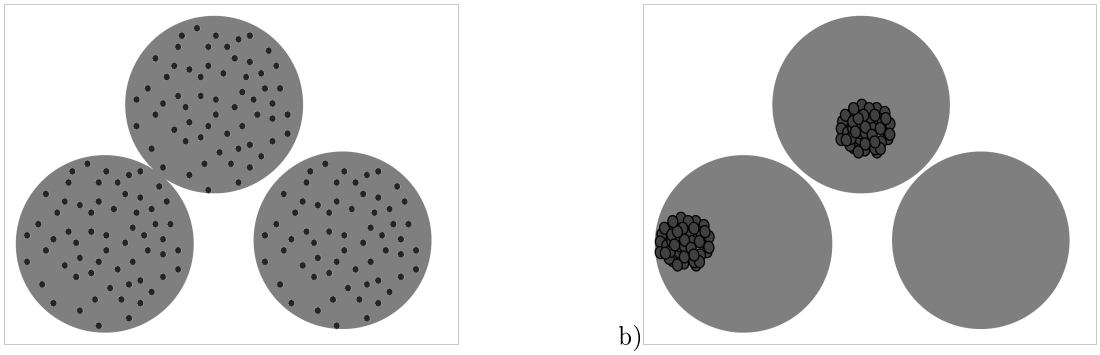

Figure 3: Visual geometries, approximately to scale for the experimental conditions in this study, 15 NTU ($30\,\frac{mg}{L}$) and $14.4\,\mu M\,Al$. a) Small aggregates (180 nm) cover 14% of the clay surface with 113 PACl aggregates per clay particle representing the control experiment described in section 2, b) Large PACl aggregates (1076 nm) cover 2.4% of the clay surface with 0.65 PACl aggregates per clay particle representing the worst case observed in this study.

The geometric analysis accounts for the observation that industrial grade PACl is not a monodisperse suspension of primary particles, but rather a suspension of preformed PACl aggregates (Malvern Zetasizer Nano-ZS). The size of these aggregates can vary greatly based on the chemical preparation techniques at the factory including aging times and handling [3, 27, 7]. The industrial grade powdered PACl used in this study (source: Zhengzhou City Jintai Water Treatment Raw Material Co., Ltd) was found to produce a suspension with an initial mean particle size of $180\,nm$ when mixed with distilled water at a concentration of $5\,mM\,Al$ (Malvern Zetasizer Nano-ZS). The fractal dimension for the preformed aggregates was estimated from the bulk density of the PACl granules as described below.

Assuming a porosity, ε, of 0.40 for random packing of spherical particles, Equation 12 was used to find the density of the preformed aggregates, $\rho_{initial}$ [5].

$$\rho_{initial} = \frac{\frac{M_{obs}}{V_{obs}}}{1-\varepsilon} \tag{12}$$

where M_{obs} is the observed mass of a dry sample of the preformed aggregates, and V_{obs} is the observed volume of the sample of preformed aggregates. The observed density, $\rho_{initial}$, was $1.138\,\frac{gm}{mL}$. Next, Equation

13 was used to calculate the number of primary particles in a single preformed aggregate, $N_{initial}$.

$$N_{initial} = \frac{\rho_{initial} * V_{initial}}{\rho_0 * V_0} \tag{13}$$

where $V_{initial}$ is the volume of a spherical preformed aggregate with a $180\,nm$ diameter, ρ_0 is the density of PACl primary particles, $1.907\,\frac{gm}{mL}$, and V_0 is the volume of a single primary particle with a $1.2\,nm$ diameter. The number of binary collisions that must have occurred to create the preformed aggregate was found by Equation 14 to be 20.9.

$$Collisions = \log_2(N_{initial}) \tag{14}$$

Finally, the fractal dimension for the factory based aggregation is determined by Equation 15.

$$D_{Fractal} = \frac{Collisions}{\log_2\left(\frac{d_{initial}}{d_0}\right)} \tag{15}$$

The resulting fractal dimension determined for the conditions observed in this study is 2.9, signifying that the PACl density was nearly independent of aggregate size in the preliminary aggregation stage during production of the PACl granules at the manufacturer. With this information, it is possible to model the fractional coverage or depth of coagulant on the surface of each clay platelet for a given set of PACl concentrations and geometric considerations. Over the range of doses in this study, increased clay surface coverage causes an increase in attachment efficiency during flocculation, which could easily explain the improvement in turbidity removal (Figure 7b). Equations 16-19 outline the calculations in the geometric model for PACl aggregate coverage of clay.

$$N_{Clay} = Influent\,Turbidity * 2\,\frac{mg}{L * NTU} * \frac{1}{M_{Clay}} \tag{16}$$

where N_{Clay} is the number of clay platelets per unit volume, $Influent\,Turbidity$ is the influent turbidity in NTU, $2\,\frac{mg}{L*NTU}$ is a conversion based on laboratory observations, M_{Clay} is the mass of each clay platelet, calculated from the volume given above and the density of kaolin clay, ρ_{Clay}, $2.65\,\frac{gm}{mL}$. The number of binary collisions that must have occurred to create an aggregate of the size dictated by the model, d_{final}, is calculated in Equation 17.

$$Collisions = D_{F,initial}\log_2\left(\frac{d_{initial}}{d_0}\right) + D_{F,final}\log_2\left(\frac{d_{final}}{d_{initial}}\right) \tag{17}$$

where $D_{F,initial}$ is the fractal dimension of the preformed aggregate, 2.9, d_0 is the diameter of the primary PACl molecule, $1.2\,nm$, $d_{initial}$ is the diameter of the preformed aggregate, $180\,nm$, $D_{F,final}$ is the fractal dimension of the aggregate, and d_{final} is the final diameter of the aggregate determined using Equation 5. $D_{F,final}$ is assumed to be equal to $D_{F,initial}$, 2.9, throughout the mixing chamber due to the high velocity gradients. The number of PACl aggregates per unit volume in the flocculator, N_{PACl}, is calculated by Equation 18.

$$N_{PACl} = \frac{C_{PACl,SRW} * N_A}{MW_{PACl} * 2^{Collisions}} \tag{18}$$

where $C_{PACl,SRW}$ is the concentration of PACl in the flocculator, N_A is Avogadro's number, and MW_{PACl} is the molecular weight of PACl. The total volume of PACl aggregates on the surface of a single clay, $V_{PAClperClay}$ is found by (Equation 19).

$$V_{PAClperClay} = \frac{V_{PACl,final} * N_{PACl}}{N_{Clay} * (1 - \varepsilon)} \tag{19}$$

where $V_{PACl,final}$ is the volume of a spherical PACl aggregate of diameter d_{final}. The total volume of the PACl aggregates is then used to determine the fractional coverage of the clay platelets. The model output is shown below (see section 3). Because PACl aggregates are assumed to be spherical, as opposed to chain-like in structure, larger aggregates have a lower surface area to volume ratio, and will require a

larger mass of coagulant to provide sufficient areal coverage of the clay platelets to obtain a high attachment efficiency. Therefore, as PACl aggregates increase in size they will be spaced further apart on the clay platelets, the attachment efficiency will decrease, and the overall particle removal efficiency in flocculation and sedimentation will decrease.

1.7. Plausible coagulation mechanisms for aggregated coagulant at low doses

The influence of coagulant dose on zeta potential is well documented in studies of the hypothesized PCN mechanism [26, 2, 9, 3]. The published data, shows that the zeta potential is not zero at the lowest residual turbidity. Results by Chu et al. [4], Wu et al. [25] show that residual turbidities drop precipitously at very low doses while the zeta potential remains negative. Similarly, efficient flocculation continues at highly positive zeta potential and the complete lack of correlation between zeta potential and residual turbidity are well documented [4]. Thus, charge neutralization does not explain the observed results and there must be another mechanism leading to enhanced attachment efficiency.

PACl self-aggregation and the absence of restabilization at positive zeta potentials demonstrates that electrostatic neutrality is not required for aggregation and confirms that the PACl-PACl attachment mechanism is stronger than the electrostatic repulsion. Therefore, although the zeta potential of the colloids becomes more positive as PACl is added to a suspension, there is no evidence that the change in zeta potential or electrostatic charge is what causes the aggregation to be successful. Therefore a different attractive force must be operative to cause aggregation of either negatively or positively charged colloids. The precise nature of the attractive force between the coagulant precipitate and other colloids is not the focus of this paper. However, it is hypothesized that trivalent cations bonded to hydroxides within the Al_{13} molecule have a strong polarity due to the large differences in electronegativity between the trivalent cation and oxygen. The atomic differences in electronegativity produce molecular level charge distributions that would provide strong intermolecular bonding. The attractive force would enable PACl to bond with itself and with clay even when there is electrostatic repulsion. If valid, this hypothesis suggests that the goal of coagulation may be to apply sufficient PACl adhesive to the colloidal particles so that a high fraction of the collision impact sites are coated with coagulant. The observed change in residual turbidity and floc size as the coagulant dose is increased may therefore be the result of the changing fractional coverage of the colloidal surfaces with the PACl adhesive. The geometric analysis given above shows that the PACl aggregates are approximately 40 (180 nm/4.2 nm) times larger than the Debye layer thickness and hence PACl aggregates extend beyond the electric double layer and electrostatic repulsion may not significantly influence the interaction between clay platelets with attached PACl aggregates.

As the geometric analysis in Figure 3 illustrates, self aggregation of PACl has a significant influence on the resulting geometry of the colloidal surfaces. If the PACl aggregate size can be kept small, then the coagulant can cover more of the colloid surface and potentially improve the attachment efficiency and turbidity removal. If the PACl is an adhesive, then the geometry of the adhesive on the colloidal surfaces is expected to influence attachment efficiency and there should be no improvement in attachment after the colloids are completely coated. The primary gain in attachment efficiency is expected to occur at low fractional coverage of the colloids.

2. Materials and methods

Experiments were conducted using an apparatus comprised of synthetic raw water and coagulant metering systems, a coiled tube hydraulic flocculator, and a flocculation residual turbidity analyzer (FReTA) (see Figure 4). Tse et al. [20] provide a complete description of the experimental apparatus and methods; only the method for coagulant addition was changed for the experimental data presented here.

Briefly, the synthetic raw water (SRW) metering system consisted of a concentrated stock suspension of kaolinite clay (R.T. Vanderbilt Co., Inc., Norwalk, CT) mixed with tap water to produce a feedback-regulated constant turbidity raw water source [22]. Reported Cornell University tap water characteristics are: total hardness $\approx 150\,\frac{mg}{L}$ as $CaCO_3$, total alkalinity $\approx 136\,\frac{mg}{L}$ as $CaCO_3$, pH ≈ 8.2, and dissolved organic carbon $\approx 1.8\,\frac{mg}{L}$ [19]. The concentrated clay stock and the SRW feedstock were each stirred to ensure homogeneous suspensions. For all of the experiments performed in this study, the SRW was maintained at a constant turbidity of 15 ± 1 NTU, which corresponded to a clay concentration of approximately $30\,\frac{mg}{L}$, and a constant temperature, $25°C$. All influent chemicals were metered with computer controlled Cole Parmer

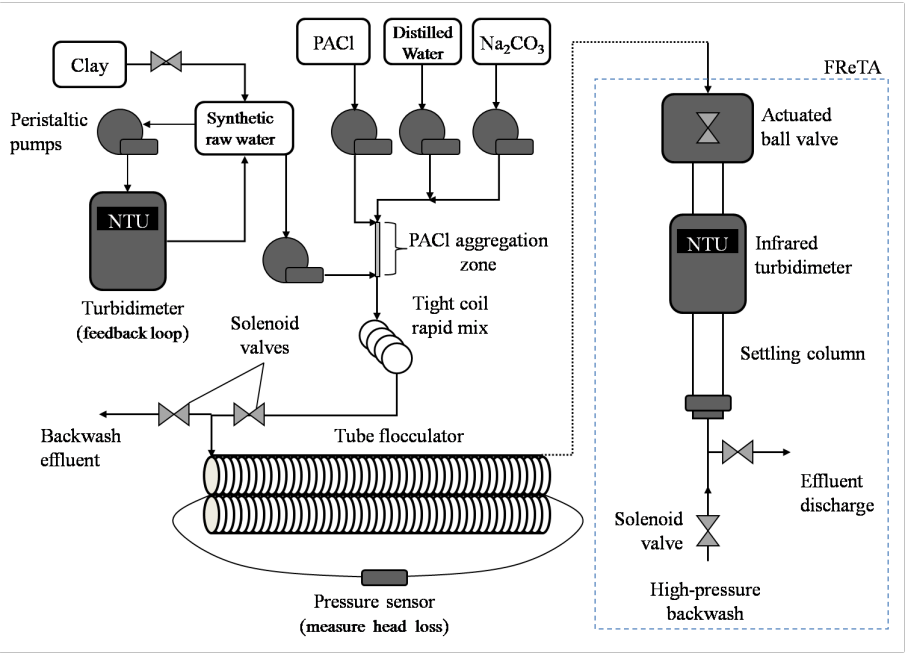

Figure 4: Schematic of the experimental assembly.

MasterFlex L/S digital peristaltic pumps. Industry grade (31% as Al_2O_3) polyaluminum chloride (PACl), $(AlO_4Al_{12}(OH)_{24}(H_2O)_{12})^{7+}$, was used as the coagulant for all experiments (Zhengzhou City Jintai Water Treatment Raw Material Co., Ltd). The PACl was diluted with distilled water to give a stock concentration of $5\,mM\,Al$. A Na_2CO_3 stock was used to neutralize the acidic PACl stock and initiate precipitation. The Na_2CO_3 stock was prepared with distilled water at a concentration of $3.43\,mM$; this concentration was chosen because with 1 to 1 mixing it adjusted the PACl stock to pH 7.5. Dilution water was prepared with distilled water and was adjusted to pH 7.5 with $75\,\mu M$ Na_2CO_3. The dilution water and Na_2CO_3 stock were combined first and then combined with the PACl stock in $0.8128\,mm$ inner diameter micro-bore tubing (Cole Parmer). The flow rate of the dilution stock was varied between experiments to alter the residence time and PACl concentration in the PACl aggregation tube (center of Figure 4).

The mixing time provided for PACl self-aggregation was determined by Equation 20.

$$t_{Mixing} = \frac{A_{Tube} * L_{Tube}}{Q_{PACl} + Q_{Na_2CO_3} + Q_{Dilution}} \tag{20}$$

where A_{Tube} is the cross-sectional area of the micro-bore tubing, $0.519\,mm^2$, L_{Tube} is the length of the micro-bore tubing, $5\,cm$ or $60\,cm$, Q_{PACl} is the flow rate of coagulant stock, $14.4\,\frac{\mu L}{s}$, found by using Equation 21, $Q_{Na_2CO_3}$ is the flow rate of base stock, $14.4\,\frac{\mu L}{s}$, and $Q_{Dilution}$ is the flow rate of pH adjusted distilled water stock, which was varied to produce a range of mixing times and concentrations. The micro-bore tubing length was either $5\,cm$ or $60\,cm$ to achieve the full range of mixing times without creating excessive head loss through the tube.

$$Q_{PACl} = \frac{PACl_{Dose} * Q_{Plant}}{PACl_{Stock}} \tag{21}$$

where Q_{Plant} is the total flow rate through the flocculator, $5\,\frac{mL}{s}$, $PACl_{Dose}$ is the concentration of PACl in the flocculator, $14.4\,\mu M\,Al$, $PACl_{Stock}$ is the concentration of PACl entering the microbore tubing, $5\,mM$.

The SRW and coagulant was passed through a rapid mix unit comprised of a $120\,cm$ segment of $4.3\,mm$ (0.17") ID tubing coiled around a cylinder with an outer diameter of 5 cm to ensure thorough mixing of the SRW and the PACl. Reynolds number in the rapid mix tube was approximately 1450. Results from a dye study showed that adequate mixing was achieved at this flow rate due to the secondary currents induced by the coiling. The coagulated SRW entered an $84\,m$ coiled tube flocculator. The average velocity gradient

in the flocculator, G, was maintained at $50\,s^{-1}$, calculated by Equations 2-9 of Tse et al. [20], and the overall plant flow rate was maintained at $5\,\frac{mL}{s}$ resulting in a hydraulic residence time, θ, of $1200\,s$ in the flocculator. As Owen et al. [18] note, flocculation is frequently studied in batch reactors with offline size measurements for aggregation processes, resulting in poor control over the energy dissipation rate, reaction time, and questionable size measurements. A tube flocculator was used because it can be idealized as a high Peclet number reactor much like a baffled hydraulic flocculator and also because the average velocity gradient in laminar tube flow is well defined [23]. After two hydraulic residence times in the flocculator, $2400\,s$, the peristaltic pumps were ramped to a stop. The FReTA actuated ball valve closed, and the turbidity in the quiescent settling column was measured over a period of 30 minutes. The flocculation residual turbidity analyzer (FReTA) was used to non-destructively measure both the sedimentation velocity and the residual turbidity of the effluent from the flocculator. The settling velocity of the particles was calculated by dividing the 13.64 cm distance between the bottom of the ball valve and the center of the zone illuminated by the turbidimeter infrared LED by the time elapsed during settling. The residual turbidity is defined as the average effluent turbidity in the fifty second interval around the capture velocity of $0.12\,\frac{mm}{s}$ which is a conservatively designed lamellar settler capture velocity [24].

Based on initial control experiments performed with the tube flocculator at $Q_{Plant} = 5\,\frac{mL}{s}$ and $G\theta = 60,000$, a coagulant dose of $14.4\,\mu M\ Al$ was determined to provide approximately 50% turbidity removal with an initial turbidity of 15 NTU (Figure 5). Residual turbidity is comprised of flocs that settle more slowly than the selected capture velocity, $0.12\frac{mm}{s}$. The $14.4\,\mu M\ Al$ dose was chosen for subsequent experiments. The sensitivity of residual turbidity to changes in coagulant addition at this dose enhanced the ability to observe changes in the effectiveness of PACl at different PACl aggregate sizes (Figure 5).

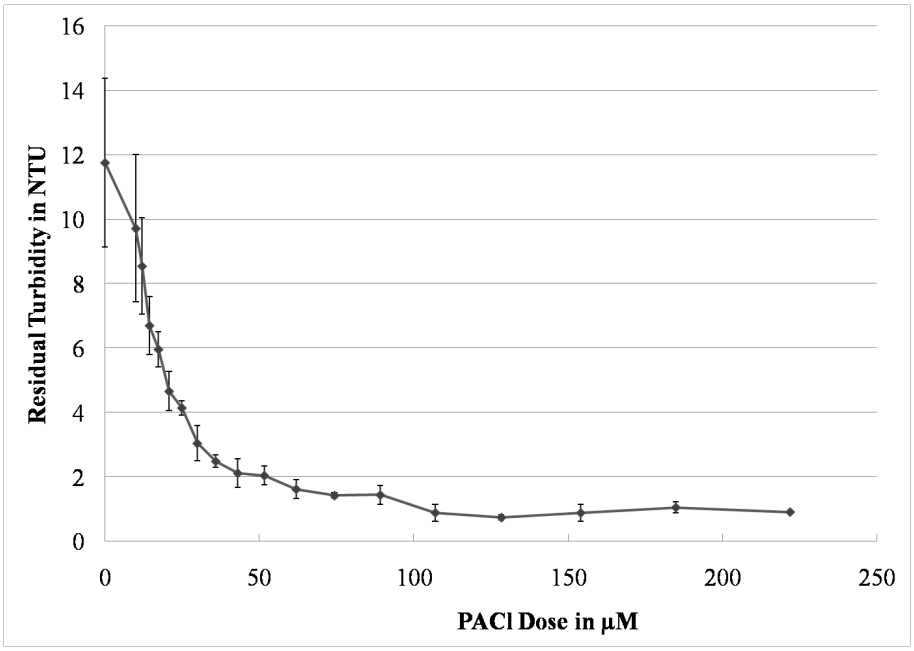

Figure 5: Control experiment used to choose the coagulant dose. Error bars represent a 95% confidence interval, n=4.

The fractional coverage of the clay by the PACl was calculated using the geometric model and the measured size of the PACl aggregates. The majority of the reduction in residual turbidity was obtained by the first 10% of clay surface coverage. There was negligible improvement in performance above a fractional coverage of approximately 40%. These results are consistent with the expectation that the effectiveness of an adhesive is related to the fractional coverage and that the significant improvement in attachment efficiency, as indirectly measured by residual turbidity, occurs when the colloids are not completely covered.

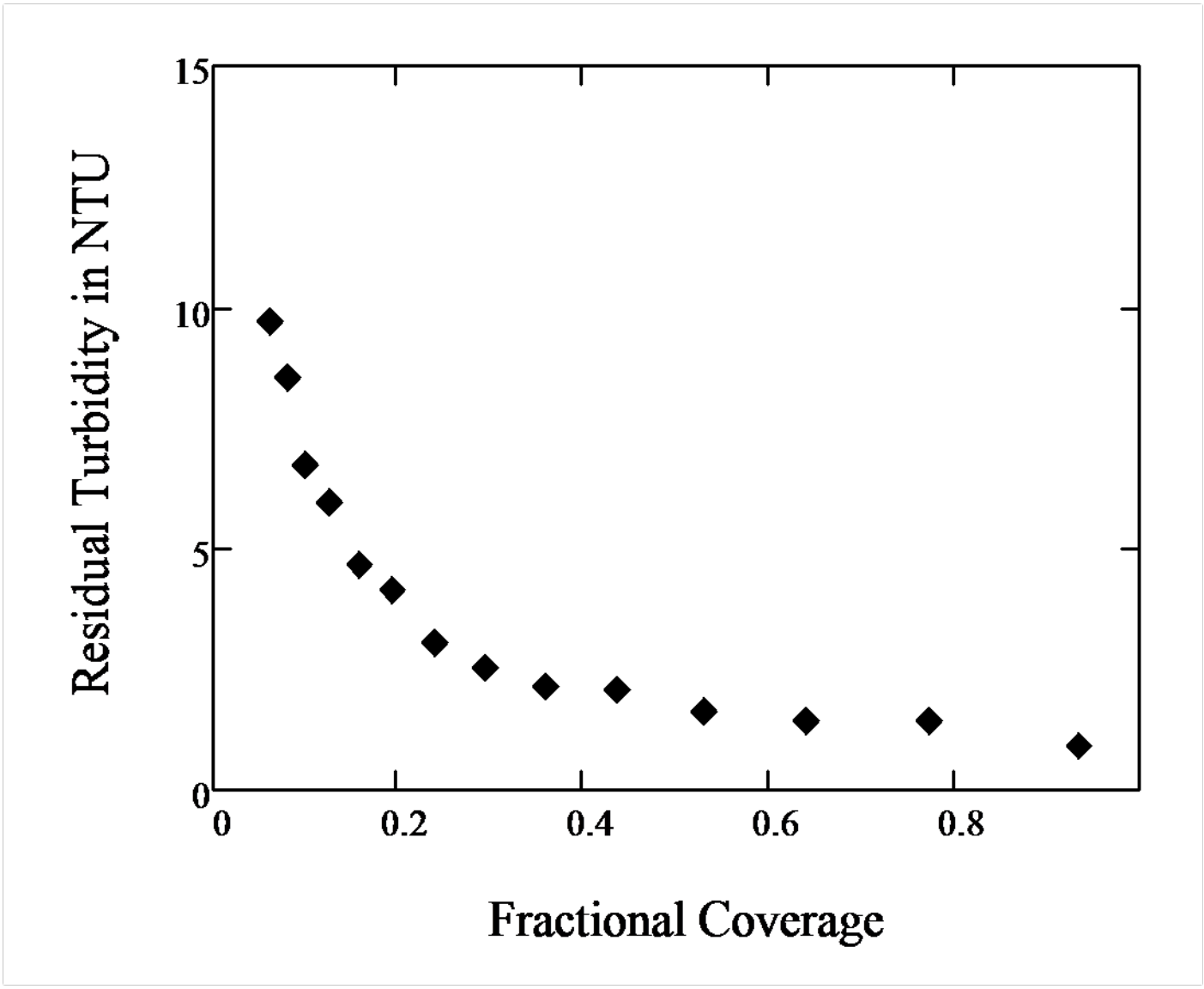

Figure 6: Residual turbidity as a function of fractional clay surface coverage by the PACl.

3. Results and discussion

The PACl aggregates ($180\,nm$ in diameter) are many times larger than the Debye length (calculated to be $4.2\,nm$ for the experimental conditions) and thus charge neutralization was not a significant factor in flocculation with powdered PACl. The geometric model and aggregation models were combined to demonstrate the potential role of clay platelet coverage on flocculation performance.

Figure 7a depicts the observed relationship between collision potential and turbidity for the tested conditions. In Figure 7d the y-axis is $pC*$, defined by Equation 22. $pC*$ is the negative logarithm of the fraction of turbidity that remains.

$$pC^* = -\log\left(\frac{Residual\,Turbidity}{Influent\,Turbidity}\right) \tag{22}$$

All calculations of size and fractional coverage incorporate a degree of uncertainty because the attachment efficiency, α, is unknown during self aggregation in the PACl mixing tube. The attachment efficiency term is expected to be low to account for curvilinear particle trajectories [6] which were not considered in the

collision model. The PACl aggregates have a high fractal dimension and a low porosity and thus flow of water through the aggregate is small and trajectory deflection as particles approach could be significant. Attachment efficiency values ranging from 0.05 to 0.2 were used to calculate the results in Figures 7b, 7c, and 7d. Assumption of higher values of α resulted in the calculation of unreasonably sized PACl aggregates (of the same order of the clay particle size). Attachment efficiencies greater than 0.1 resulted in fewer than 1 PACl aggregate per clay particle and is thus inconsistent with the observed flocculation and sedimentation.

Because mixing time was varied by the addition of dilution water, concentration of PACl in the PACl aggregation tube varied in each test. The parameter $G\theta\phi^{2/3}$, where G is the velocity gradient, θ is the mixing time or residence time in the PACl aggregation tube, and ϕ is the initial floc volume fraction, was chosen to represent collision potential in the mixing tube in accordance with Weber-Shirk and Lion [23]. Since longer mixing times and higher PACl concentrations allow more PACl self-aggregation, the experimental results can also be expressed as a function of model-calculated PACl aggregate size as shown in Figure 7b. It is clear that the performance of PACl as a coagulant is impaired by the formation of large PACl aggregates. Given the diameter of model-calculated PACl aggregates, the surface coverage of kaolin clay colloids can be calculated (Equation 23) and is shown in Figure 7c. For a constant PACl dose, increased aggregate size results in fewer PACl aggregates per clay, which in turn correlates with the decrease in fractional removal shown in Figure 7d.

$$Fractional\,Coverage = \frac{V_{PAClperClay}}{SA_{Clay} * d_{final}} \tag{23}$$

where SA_{Clay} is the surface area of a single clay platelet and $V_{PAClperClay}$ is the total volume of PACl aggregates per clay platelet given by Equation 19.

The data collected from FReTA in each of these experiments can be used to calculate the distribution of sedimentation velocities for the flocs formed under the given conditions. Figure 8 shows turbidity as a function of sedimentation velocity for a sample of the aggregate sizes in the study, assuming $\alpha = 0.1$ to estimate the PACl aggregate sizes given in the legend. The sedimentation velocity is strongly correlated to the final floc size and determines the probability that a floc is removed. The slope of the curve represents the fraction of the flocs with the corresponding sedimentation velocity. Residual turbidity is comprised of flocs that settle more slowly than the capture velocity of a conservatively designed lamellar settler in a sedimentation tank, $0.12\,\frac{mm}{s}$ in these experiments. Figure 8 shows that the fraction of particles with settling velocities lower than $0.12\,\frac{mm}{s}$ increased at larger PACl aggregate sizes.

Starting with $180\,nm$ initial aggregates, formation of a $1076\,nm$ PACl aggregate requires approximately 6.2 seconds in the mixing chamber assuming a self-aggregation attachment efficiency of 0.1. As shown in Figure 7a, providing PACl time for self-aggregation will decrease the performance of the subsequent flocculation process by decreasing the attachment efficiency in the floccualtion phase andincreasing residual turbidity. Therefore, rapid mixing of coagulant with colloid suspensions after coagulant addition is needed to ensure PACl does not self-aggregate before contacting colloids in the water to be treated. PACl will begin to self-aggregate as soon as the PACl stock blends with sufficient raw water to neutralize the pH of the mixture. The dilution required to begin self-aggregation is a function of the acid neutralizing capacity (ANC) of the PACl stock and the ANC and pH of the raw water. Self-aggregation will occur most readily for high pH and high ANC waters such as raw waters in equilibrium with calcium carbonate. Self-aggregation is also favored by high PACl dose and low raw water colloid concentration because the distance between PACl aggregates would be small and the probability of first colliding with a PACl over a clay platelet would be enhanced. If mixing does not occur at the point of coagulant application, the pH of the PACl stock will be neutralized upon entering the water and the local concentration of coagulant will remain high leading to self-aggregation. Self-aggregation after complete mixing with the raw water is expected to be insignificant because PACl aggregate interactions with clay platelets become highly favored over self-aggregation.

While rapid mix of coagulant with raw water has been a prerequisite to flocculation for decades, the results of this study suggest that coagulation with PACl requires immediate, rapid mixing to decrease the local concentration of coagulant at the point of addition. Although beyond the scope of the present study, mixing also aids in the uniform application of the PACl aggregates on the raw water colloid surfaces.

4. Conclusions

1. Electrostatic charge neutralization is not required for PACl coagulation because the PACl aggregates are much larger than the Debye length scale.
2. Geometric considerations show the reduction in residual turbidity as a function of PACl dose occurs over a dose range that is consistent with partial clay platelet coverage with adhesive PACl aggregates.
3. PACl will readily precipitate and aggregate at circum-neutral pH in short time scales (~5 s) to sizes that are significant to the performance of the whole water treatment plant.
4. At a constant dose, increased size of PACl aggregates decreases clay surface coverage and negatively affects the performance of subsequent flocculation and sedimentation processes.
5. PACl self-aggregation is not expected to be a factor in municipal water treatment plants once the coagulant is uniformly mixed with the raw water.

The quantitative turbidity removal - PACl aggregation relationships observed in this research are specific to the experimental test conditions and are expected to vary in magnitude with influent water quality and coagulant dose. However, the qualitative effect of coagulant self-aggregation can be generalized and it is clear that PACl aggregate size is a characteristic that should be considered when evaluating the results of flocculation performance experiments. From the perspective of the practical application of PACl to water treatment, this research shows that turbidity removal by flocculation and sedimentation is improved if vigorous mixing occurs at the point of PACl addition. Immediate mixing with a high energy dissipation rate, ε, will increase the separation distance between PACl aggregates and increase the probability that the closest particle which the PACl will attach to is a clay particle, as opposed to another PACl aggregate. Some methods of coagulant addition such as a drip feed into an entrance tank of standing water are expected to not be effective means for rapid dispersal of coagulant. These dosing methods are anticipated to allow self-aggregation of coagulant and necessitate a higher coagulant dose than would be needed if efficient mixing were achieved.

5. References

[1] D. Asnaghi, M. Carpineti, M. Giglio, and M. Sozzi. Coagulation kinetics and aggregate morphology in the intermediate regimes between diffusion limited and reaction limited cluster aggregation. *Physical Review A (Statistical Physics, Plasmas, Fluids, and Related Interdisciplinary Topics)*, 45(2):1018–23, January 1992.

[2] David Bache and Ross Gregory. *Flocs in Water Treatment*. IWA Publishing, London, UK, 2007.

[3] J. E. Van Benschoten and J. K. Edzwald. Chemical aspects of coagulation using aluminum salts - i. hydrolytic reactions of alum and polyaluminum chloride. *Water research*, 24(12):1519–1526, 1990.

[4] YongBao Chu, BaoYu Gao, QinYan Yue, and Yan Wang. Investigation of dynamic processing on aluminum floc aggregation: Cyclic shearing recovery and effect of sulfate ion. *Science in China Series B: Chemistry*, 51(4):386–392, 2008.

[5] R. M. German. Particle packing characteristics. Technical report, Metal Powder Industries Federation, 1989.

[6] D. W. Hendricks. *Fundamentals of Water Treatment Unit Processes: Physical, Chemical, and Biological*. Taylor and Francis, 2009. ISBN 9781420061918. URL `http://books.google.com/books?id=9QNtn0P6fkwC`. 2010036943.

[7] Chengzhi Hu, Huijuan Liu, and Jiuhui Qu. Preparation and characterization of polyaluminum chloride containing high content of al13 and active chlorine. *Colloids and Surfaces A- Physicochemical and Engineering Aspects*, 260(1-3):109–117, 6 2005.

[8] Hang Li, Shiqiang Wei, Changle Qing, and Jinshan Yang. Discussion on the position of the shear plane. *Journal of colloid and interface science*, 258(1):40–44, February 2003.

[9] Tao Li, Zhe Zhu, Dongsheng Wang, Chonghua Yao, and Hongxiao Tang. The strength and fractal dimension characteristics of alum - kaolin flocs. *International Journal of Mineral Processing*, 82(1): 23–29, 2 2007.

[10] Jr-Lin Lin, Ching-Ju M. Chin, Chihpin Huang, Jill R. Pan, and Dongsheng Wang. Coagulation behavior of al13 aggregates. *Water research*, 42(16):4281–4290, 2008.

[11] Jr-Lin Lin, Chihpin Huang, Ching-Ju M. Chin, and Jill R. Pan. Coagulation dynamics of fractal flocs induced by enmeshment and electrostatic patch mechanisms. *Water research*, 42(17):4457–4466, 11 2008.

[12] Jr-Lin Lin, Chihpin Huang, Ching-Ju M. Chin, and Jill R. Pan. The origin of al(oh)3-rich and al13-aggregate flocs composition in pacl coagulation. *Water research*, 43(17):4285–4295, 9 2009.

[13] M. Y. Lin, H. M. Lindsay, D. A. Weitz, R. C. Ball, R. Klein, and P. Meakin. Universal reaction-limited colloid aggregation. *Physical Review A (Statistical Physics, Plasmas, Fluids, and Related Interdisciplinary Topics)*, 41(4):2005–20, 02/15 1990.

[14] Po-Hsun Lin, Monroe L. Weber-Shirk, and Leonard W. Lion. Comparison of the ability of three coagulants to enhance filter performance. *ASCE Journal of Environmental Engineering*, (accepted for publication), 2010.

[15] Majid Emami Meibodi, Mohsen Vafaie-Sefti, Ali Morad Rashidi, Azadeh Amrollahi, Mohsen Tabasi, and Hossein Sid Kalal. Simple model for thermal conductivity of nanofluids using resistance model approach. *International Communications in Heat and Mass Transfer*, 37(5):555–559, 5 2010.

[16] Jun Nan, Weipeng He, Juanjuan Song, and Xinxin Song. Fractal growth characteristics of flocs in flocculation process in water treatment. In *2009 International Conference on Energy and Environment Technology (ICEET 2009)*, volume 2, pages 582–8, Piscataway, NJ, USA, October 2009. State Key Lab. of Urban Water Resource Environ., Harbin Inst. of Technol., Harbin, China, IEEE.

[17] C. R. O'Melia, K. A. Gray, and C. Yao. Polymeric inorganic coagulants. Technical report, American Water Works Association, December 1989 1989.

[18] A. T. Owen, P. D. Fawell, J. D. Swift, D. M. Labbett, F. A. Benn, and J. B. Farrow. Using turbulent pipe flow to study the factors affecting polymer-bridging flocculation of mineral systems. *International Journal of Mineral Processing*, 87(3-4):90–99, July 2008.

[19] Bolton Point Water System. Drinking water quality report 2011. Technical report, Southern Cayuga Lake Intermunicipal Water Commission, 2011.

[20] Ian C. Tse, Karen Swetland, Monroe L. Weber-Shirk, and Leonard W. Lion. Method for quantitative analysis of flocculation performance. *Water research*, 45(10):3075–3084, 5 2011.

[21] C. J. van Oss, R. F. Giese, and P. M. Costanzo. Dlvo and non-dlvo interactions in hectorite. *Clays and Clay Minerals*, 38(2):151–159, 1990.

[22] M. L. Weber-Shirk. An automated method for testing process parameters, 2008.

[23] Monroe L. Weber-Shirk and Leonard W. Lion. Flocculation model and collision potential for reactors with flows characterized by high peclet numbers. *Water research*, 44(18):5180–5187, 10 2010.

[24] Roderick M. Willis. Tubular settlers a technical review. *Journal AWWA*, June:331–335, 1978.

[25] Xiaohong Wu, Xiaopeng Ge, Dongsheng Wang, and Hongxiao Tang. Distinct coagulation mechanism and model between alum and high al13-pacl. *Colloids and Surfaces A: Physicochemical and Engineering Aspects*, 305(1-3):89–96, September 2007.

[26] Xiaohong Wu, Xiaopeng Ge, Dongsheng Wang, and Hongxiao Tang. Distinct mechanisms of particle aggregation induced by alum and pacl: Floc structure and dlvo evaluation. *Colloids and Surfaces A: Physicochemical and Engineering Aspects*, 347(1-3):56–63, 2009.

[27] Mingquan Yan, Dongsheng Wang, Jinren Ni, Jiuhui Qu, Christopher W. K. Chow, and Hailong Liu. Mechanism of natural organic matter removal by polyaluminum chloride: Effect of coagulant particle size and hydrolysis kinetics. *Water research*, 42(13):3361–3370, 2008.

[28] Changqing Ye, Dongsheng Wang, Baoyou Shi, Jianfeng Yu, Jiuhui Qu, Marc Edwards, and Hongxiao Tang. Alkalinity effect of coagulation with polyaluminum chlorides: Role of electrostatic patch. *Colloids and Surfaces A: Physicochemical and Engineering Aspects*, 294(1-3):163–173, 2007.

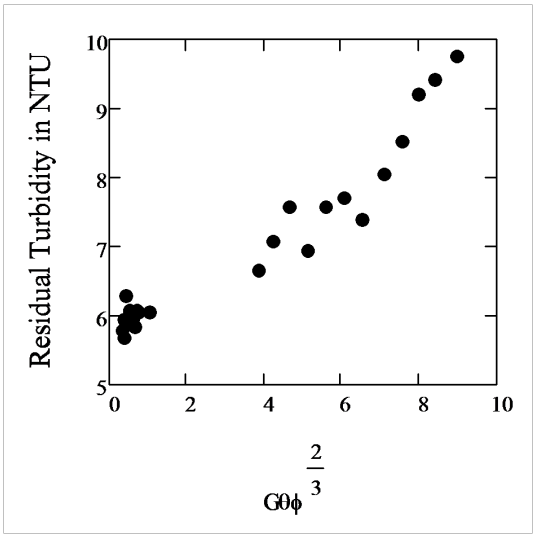

(a) Residual turbidity as a function of collision potential in the PACl aggregation tube, $G\theta\phi^{2/3}$.

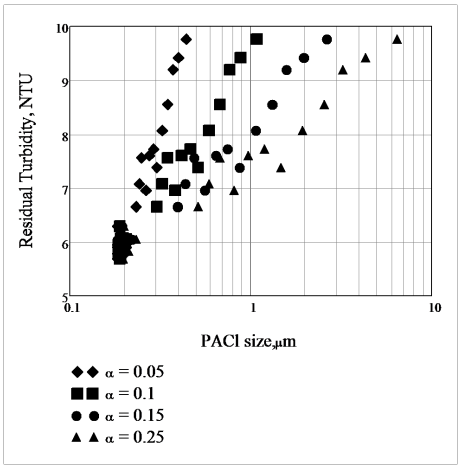

(b) Residual Turbidity as a function of PACl aggregate size for 4 assumed attachment efficiencies.

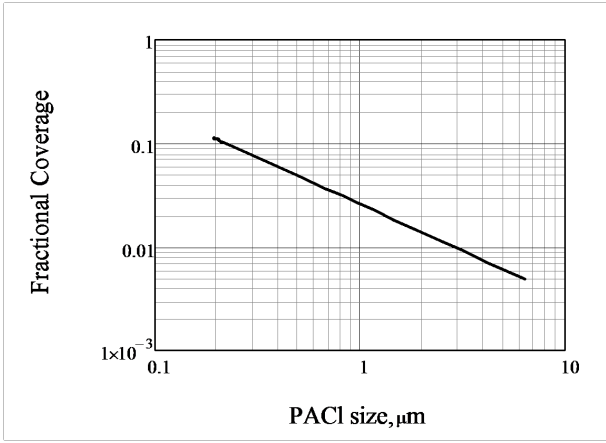

(c) Surface coverage as a function of PACl aggregate size.

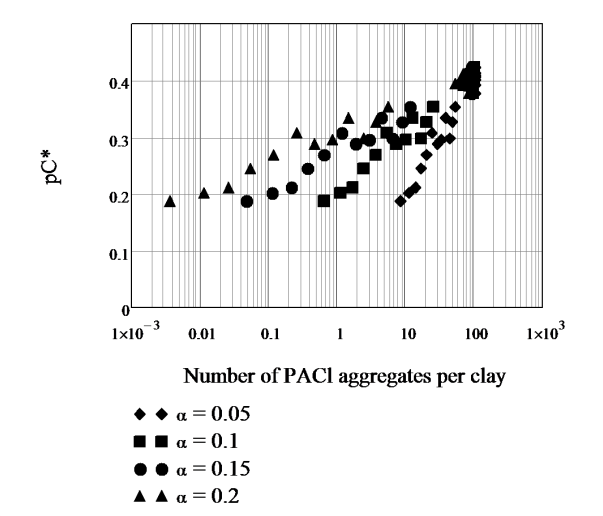

(d) Observed pC* as a function of the number of PACl aggregates per clay.

Figure 7: Influent turbidity was 15 NTU, PACl dose was $14.4\,\mu M\ Al$ for all points. Initial PACl aggregate size of $180\,nm$ estimated for the model.

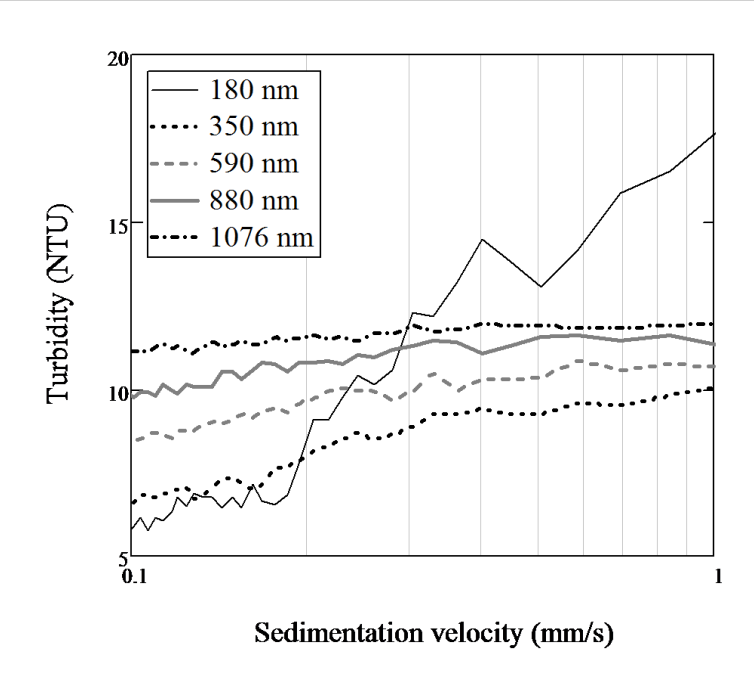

Figure 8: Sedimentation velocity from PACl aggregates of various sizes. The vertical line represents the capture velocity, the sedimentation velocity at which the residual turbidity measurement is taken. Data was collected at 1 second intervals for 30 minutes of settling. Each plot consists of 50 data points, each an average of 36 seconds of data.